International Journal of Modern Physics A
Vol. 34, No. 29 (2019) 1950169 (13 pages)

DOI: 10.1142/S0217751X19501690

Excited quarks production at FCC and S*pp*C *pp* colliders

Mehmet Sahin
Department of Physics, Usak University, Usak, Turkey
mehmet.sahin@usak.edu.tr

Güral Aydin
Department of Physics, Hatay Mustafa Kemal University, Hatay, Turkey
gaydin@mku.edu.tr

Yusuf Oguzhan Günaydin*
Department of Physics, Kahramanmaras Sütcü Imam University,
Kahramanmaras, Turkey
yusufgunaydin@gmail.com

Received 2 August 2019
Revised 28 September 2019
Accepted 29 September 2019
Published 23 October 2019

Potential discovery, observation and exclusion limits of excited u and d quarks with gamma + jet final state are researched at the multi-TeV scale colliders, FCC and S*pp*C in this paper. Both colliders, FCC and S*pp*C, show that excited u and d quarks could be discovered up to 42.1 TeV and 55.2 TeV for $u^\star$, 30.3 TeV and 39.4 TeV for $d^\star$ and 42.3 TeV and 55.5 TeV mass values for degenerate case ($m_{u^\star} = m_{d^\star}$), respectively. The determination of the excited quarks compositeness scale is examined, which will be up to multi-PeV level. Besides these analyses, free parameters (f_s, f and f') are scanned from around 0.1 up to 1 that show excited quark could be discovered at dozens of TeV with even coupling constants under 0.1.

Keywords: Excited quarks; preonic models; FCC; S*pp*C; compositeness scale.

PACS numbers: 12.60.Rc, 14.80.−j

1. Introduction

The historical development of the elementary particles[1] suggest that there could be more fundamental particles than Standard Model (SM) fermions. Therefore, over

*Corresponding author.

the last four decades, both experimental and theoretical particle physicists have proposed new models claiming that SM fermions could have composite substructure, which is called preons.[2–13] Preonic interactions bring into such new hypothetical particles like diquarks, dileptons, leptogluons, leptoquarks, excited quarks ($Q^\star$) and excited leptons ($l^\star$). As a matter of fact, in the SM, there should be three possible families for excited fermions. This paper focuses on the analysis of the first family spin-1/2 excited quarks ($u^\star$ and $d^\star$). The existence of the excited quark will be robust verification of such a state that the composite structure of the fundamental particle might be possible. Excited quark mass is expected to be much more massive than the SM quark mass.

The LHC working plan will end in the 2020s, and more energetic particle colliders are required to observe and discover these unstable and heavy particles. After that, two new energy-frontier particle collider machines, Future Circular Collider (FCC) at CERN and Super Proton–Proton Collider (SppC) in China, are planned for the extensive investigation on hypothetical particles. FCC's working plan will be carried out in two phases. It is expected to reach its final integrated luminosity as 2.5 ab^{-1} at phase I in 10 years and 15 ab^{-1} at phase II in 15 years. Overall, the integrated luminosity of the FCC is expected as 17.5 ab^{-1} in 25 years.[14] On the other hand, SppC is presumed to reach 22.5 ab^{-1} in 15 years.[15–17]

There are some experimental[18–32] and phenomenological[2–13,33–65] research that investigate excited fermions and provide mass limits of excited quarks based on final state particles. Currently, CERN LHC collaborations (ATLAS and CMS) hold experimental exclusion limits on excited quark mass in proton–proton collisions as $m_{q^\star} = 6.0$ TeV at jj, $m_{q^\star} = 5.5$ TeV at γj final states according to both experiments, and $m_{q^\star} = 3.2$ TeV at Wj and $m_{q^\star} = 2.9$ TeV at Zj final states for the ATLAS experiment, $m_{q^\star} = 5.0$ TeV at Wj and $m_{q^\star} = 4.7$ TeV at Zj final states for the CMS experiment.

In this research, we analyzed production cross-section of spin-1/2 excited u and d quark ($u^\star$ and $d^\star$) decaying into gamma + jet final states at the FCC and the SppC with their expected integrated luminosities. The following section presents the interaction Lagrangian of spin-1/2 excited quark and its decay widths. Then, cross-section values in Sec. 3, signal-background analysis to determine cuts in Sec. 4, and attainable mass, compositeness scale (Λ) limits, free parameters' scan and conclusions in Sec. 5 are introduced.

2. Interaction Lagrangian of Spin-1/2 Excited Quarks and Decay Widths

The first generation SM and excited quarks' isospin structure are described by[44]

$$\begin{bmatrix} u \\ d \end{bmatrix}_L , \; u_R \, d_R \, , \; \begin{bmatrix} u^\star \\ d^\star \end{bmatrix}_L , \; \begin{bmatrix} u^\star \\ d^\star \end{bmatrix}_R .$$

Interaction Lagrangian of spin-1/2 excited quarks, which interact with SM gauge bosons and quarks, is presented in Eq. (1). Here, Λ represents compositeness scale, $Q_R^\star$ is right-handed excited quark, Q_L is SM quark, g_s, g and g' are gauge coupling constants, $F^a_{\mu\nu}$, $\mathbf{W}_{\mu\nu}$, $B_{\mu\nu}$ are the field strength tensors for gluon, SU(2) and U(1), λ^a are 3×3 Gell-Mann matrices, $\boldsymbol{\tau}$ is the Pauli spin matrices, $Y = 1/3$ is weak hypercharge and f_s, f and f' are dimensionless free parameters specified by compositeness dynamics, which state the strength of the excited quarks couplings to their SM associates and are all generally assumed to be of order unity. Equation (1) has been implemented to CalcHEP[66] simulation software via LanHEP,[67,68]

$$L_{\text{eff}} = \frac{1}{2\Lambda}\,\overline{Q_R^\star}\,\sigma^{\mu\nu}\left[g_s f_s \frac{\lambda_a}{2} F^a_{\mu\nu} + g f\,\frac{\boldsymbol{\tau}}{2}\mathbf{W}_{\mu\nu} + g' f'\,\frac{Y}{2} B_{\mu\nu}\right] Q_L + \text{h.c.} \qquad (1)$$

The analytical formulae for excited up- and down-quark partial decay width are presented in Eqs. (2)–(4). In these equations, SM quark mass is neglected because the experimental limits on excited quark mass are at TeV scales:[24,25]

$$\Gamma_{(Q^\star \to Qg)} = \frac{1}{3}\alpha_s f_s^2 \frac{m_{Q^\star}^3}{\Lambda^2}\,, \qquad (2)$$

$$\Gamma_{(Q^\star \to Q\gamma)} = \frac{1}{4}\alpha f_\gamma^2 \frac{m_{Q^\star}^3}{\Lambda^2}\,, \qquad (3)$$

$$\Gamma_{(Q^\star \to QV)} = \frac{1}{32\pi} g_V^2 f_V^2\,\frac{m_{Q^\star}^3}{\Lambda^2}\left(1 - \frac{m_V^2}{m_{Q^\star}^2}\right)^2 \left(2 + \frac{m_V^2}{m_{Q^\star}^2}\right), \qquad (4)$$

where V denotes W or Z bosons, Q represents u or d quarks and $Q^\star$ symbolizes $u^\star$ or $d^\star$ excited quarks and then considering T_3 is the third component of weak isospin and Y is weak hypercharge of an excited quark; $f_\gamma = fT_3 + f'(Y/2)$, $f_Z = fT_3 \cos^2\theta_W - f'(Y/2)\sin^2\theta_W$, $f_W = f/\sqrt{2}$.

The decay width values obtained via CalcHEP are summarized in Fig. 1. Total and partial decay widths for $u^\star$ and $d^\star$ are examined starting from 5.5 TeV to 100 TeV mass ranges with $f = f_s = f' = 1$. Besides two different flavors used in analysis, decay widths are plotted in terms of different compositeness values. In Fig. 1, compositeness scale was chosen 100 TeV in the first row and it was selected equal to excited quark mass in the second row.

It is apparent from Fig. 1 that $Q^\star \to \gamma + Q$ channel makes the lowest contribution to total decay width unlike $Q^\star \to g + Q$ channel. While the latter channel corresponds to dijet final states, the former channel corresponds to gamma + jet final state, which has a lower background than the dijet final state. Therefore, we focused on gamma + jet final state in this work.

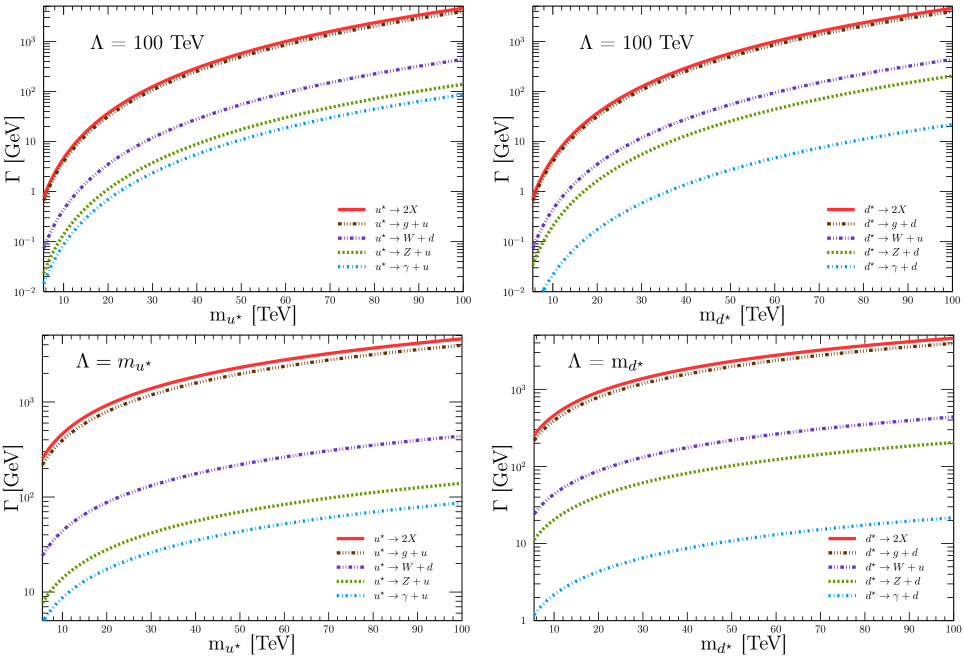

Fig. 1. Partial and total decay widths for $u^\star$ (left panel) and $d^\star$ (right panel).

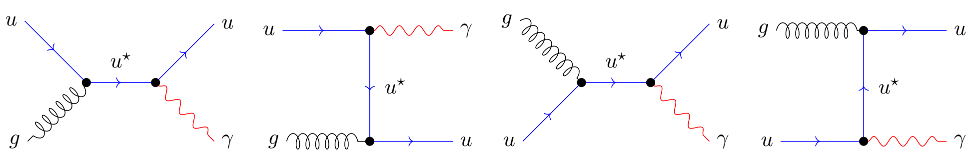

Fig. 2. Illustration of signal process Feynman diagrams for direct and indirect production at *pp* colliders.

3. Excited Quarks Production Cross-Sections at Multi-TeV Scale

In this paper, three different cases as the signal process, which are listed in Eq. (5) are considered to be studied where $q^\star$ means $u^\star + d^\star$. Firstly, production cross-section values are computed via CalcHEP simulation software in which cross-section plots (Fig. 3) are generated by using CTEQ6L1[69,70] quark distribution function and taking renormalization and factorization scales equal to excited quark masses. At proton–proton colliders, resonance production of excited quarks cross-section values obtained at leading-order (LO) level are as high as next-to-leading order (NLO) level cross-section values due to resonance production of excited quarks via quark–gluon fusion. Therefore, LO level cross-section values are used in experimental studies without computation of any k-factor[21,54,71] for excited quarks. So, all calculations are done at a LO level. According to LHC experiments[25,29] using different selections of PDF, factorization and renormalization scales cause less than 1% contribution on systematic uncertainties for $Q^\star \to \gamma Q$ channel.

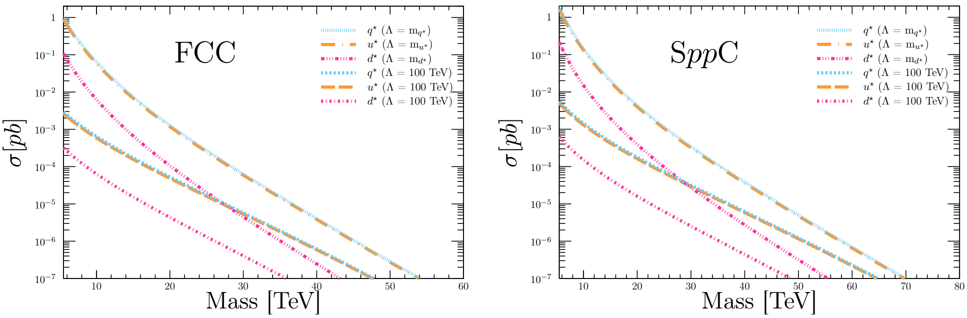

Fig. 3. $q^\star$, $u^\star$ and $d^\star$ cross-section values for the FCC (left panel) and SppC (right panel).

Figure 2 illustrates four Feynman diagrams that contribute to signal cross-section for the case described in Eq. (5a). Besides these diagrams, cases described in Eqs. (5b) and (5c) contribute to signal cross-section with four and eight Feynman diagrams, respectively.

$$m_{u^\star} > m_{d^\star} \quad \text{for} \quad pp \to u^\star + X \to \gamma u + X\,, \tag{5a}$$

$$m_{d^\star} > m_{u^\star} \quad \text{for} \quad pp \to d^\star + X \to \gamma d + X\,, \tag{5b}$$

$$m_{u^\star} = m_{d^\star} \quad \text{for} \quad pp \to q^\star + X \to \gamma q + X \ \text{(degenerate state)}\,. \tag{5c}$$

As shown in Fig. 3, excited u-quark cross-section values are significantly higher than excited d-quark due to proton's two valence up quarks and electric charge difference of excited up (2/3) and down (−1/3) quarks. It is roughly estimated that for ten events, $u^\star$ and $d^\star$ can be produced up to 46 TeV, 36 TeV mass limits at FCC and 58 TeV and 45 TeV at SppC, respectively.

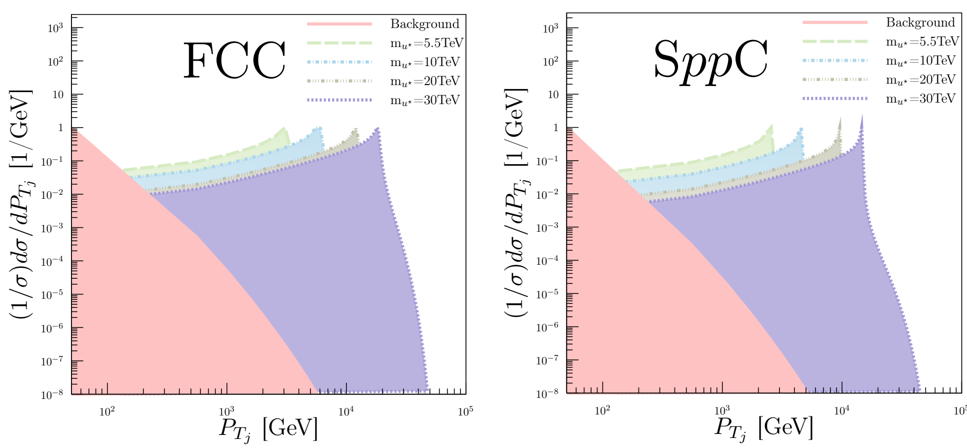

Fig. 4. $u^\star$ transverse momentum distribution plots for the FCC (left panel) and SppC (right panel).

4. Signal Background Analysis of Excited Quarks

As it is declared in the previous section, three signal processes, $pp \to u^\star + X \to \gamma u + X$, $pp \to d^\star + X \to \gamma d + X$ and $pp \to q^\star + X \to \gamma q + X$ (degenerate state) are analyzed along with background process $pp \to \gamma j + X$. Here, j indicates u, $\bar{u}$, d, $\bar{d}$, c, $\bar{c}$, s, $\bar{s}$, b, $\bar{b}$, and g. Transverse momentum and pseudorapidity distributions that depending on normalized differential cross-sections are plotted for both colliders by considering four different signal mass values with gamma + jet final state.

Transverse momentum (P_T), pseudorapidity (η_j or η_γ) and invariant mass ($m_{\gamma j}$) cuts that distinguish the signal process from the background process are implemented. Both final state particle transverse momentum distributions show almost the same characteristic. For this reason, one distribution plot is presented for illustration. As shown in Fig. 4, 2000 GeV cut significantly reduces the background while the signal remains almost unchanged. This cut is far beyond the experimental P_T

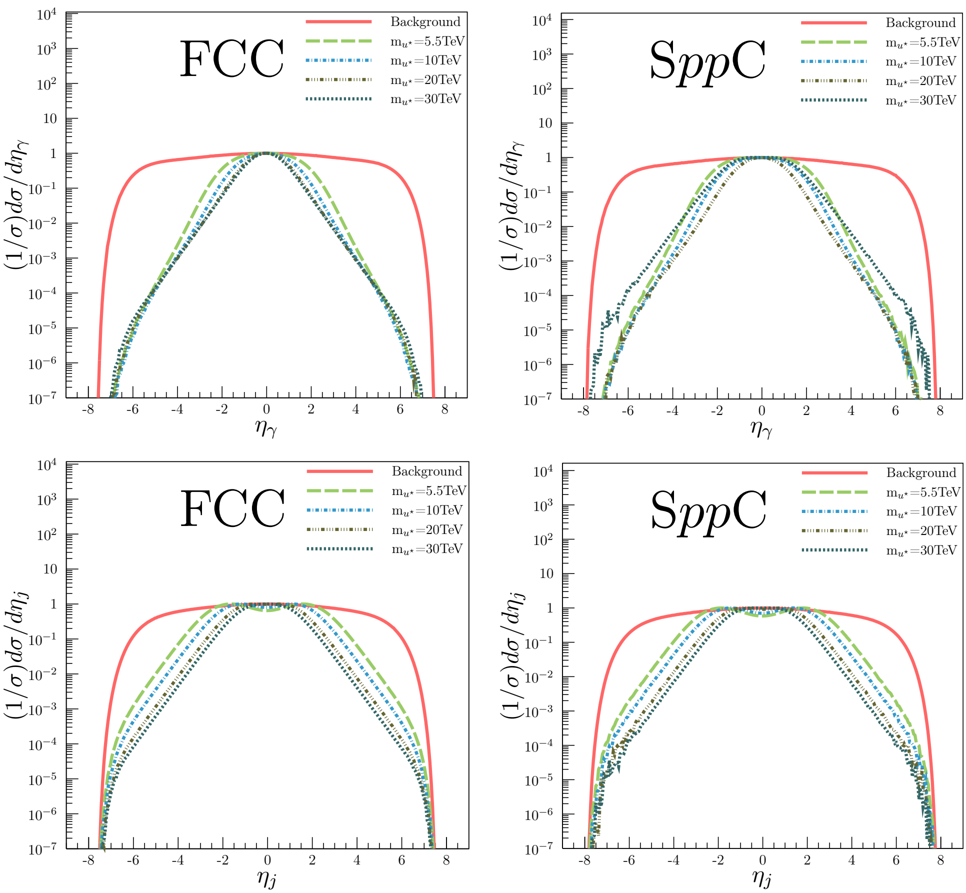

Fig. 5. $u^\star$ pseudorapidity distribution plots for the FCC (left panel) and S*pp*C (right panel) at γ (first row) and jet (second row) final states.

cut because if $P_T > 150$ GeV and events contain at least one photon and one jet candidate, photon and jet registration is nearly 100%.[25] Pseudorapidity regions are selected between -2.5 and 2.5 for jet and between -1.44 and 1.44 for photon based in Fig. 5.

The invariant mass cut is applied as $m^\star - 2\Gamma^\star < m_{\gamma j} < m^\star + 2\Gamma^\star$ mass window, here $m^\star$ indicates excited quark mass and $\Gamma^\star$ denotes total decay width of corresponding excited quark. Additionally, to differentiate photon and jet, the cone angle radius (ΔR) cut is used as $\Delta R > 0.5$

$$S_{\text{stat}} = \frac{\sigma_s}{\sqrt{\sigma_s + \sigma_b}} \sqrt{\mathcal{L}_{\text{int}}}\,. \tag{6}$$

To obtain statistical significance values, Eq. (6) is utilized, where σ_s depicts signal cross-section, σ_b means background cross-section and $\mathcal{L}_{\text{int}}$ is integrated luminosity. By using this formula, all confidence levels, discovery (5σ), observation (3σ),

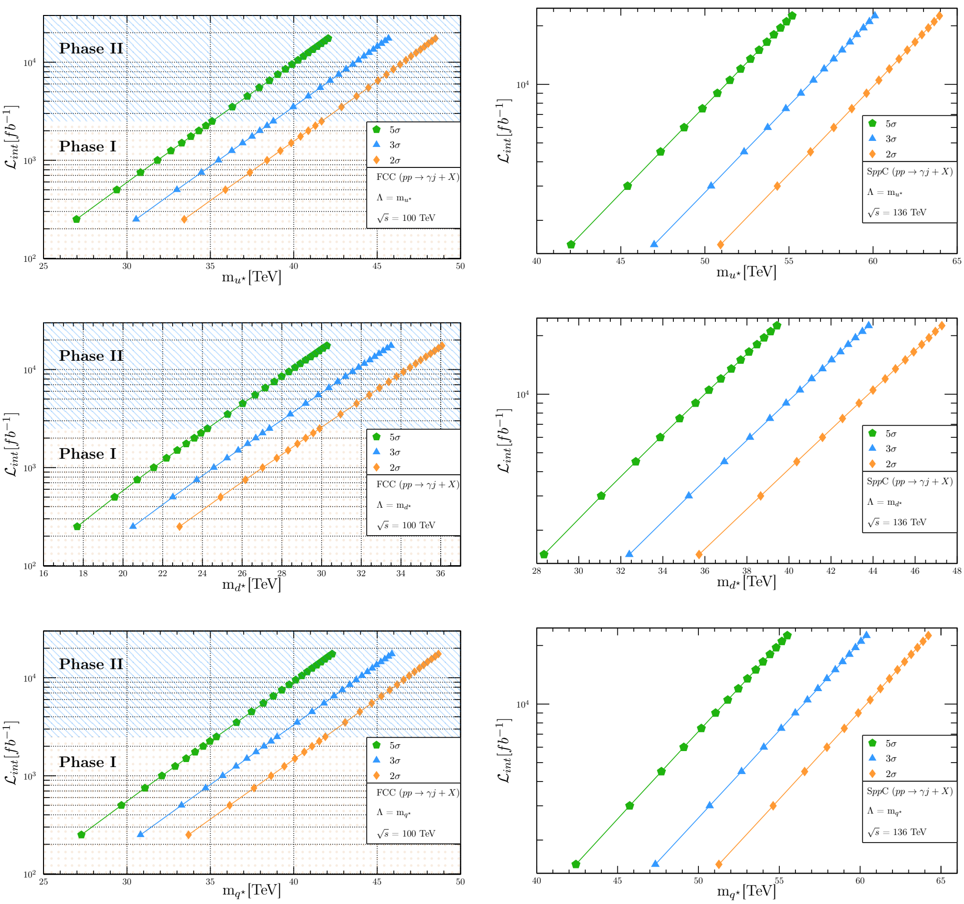

Fig. 6. Luminosity mass plots for the FCC (left panel) and SppC (right panel).

and exclusion (2σ) are computed with applied cuts as mentioned above for FCC and SppC colliders.

5. Results and Conclusions

In this analysis, excited quark mass limits depending on integrated luminosity are calculated by implementing cut values and utilizing statistical significance formula mentioned in the previous section for both collider options. These limits are presented in Fig. 6 based on expected operation time of FCC and SppC colliders. Excited quarks' discovery (5σ), observation (3σ), and exclusion (2σ) mass limits

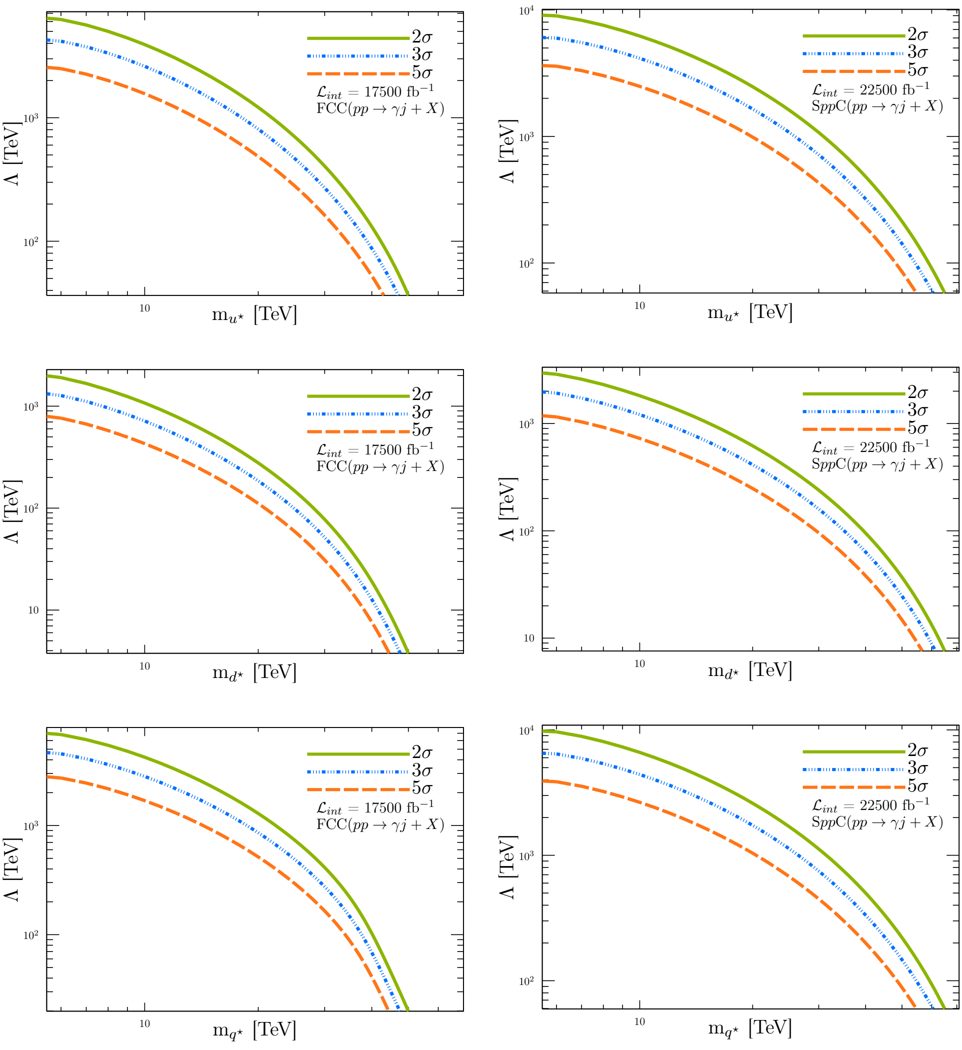

Fig. 7. Compositeness scale-mass plots for the FCC (left panel) and SppC (right panel).

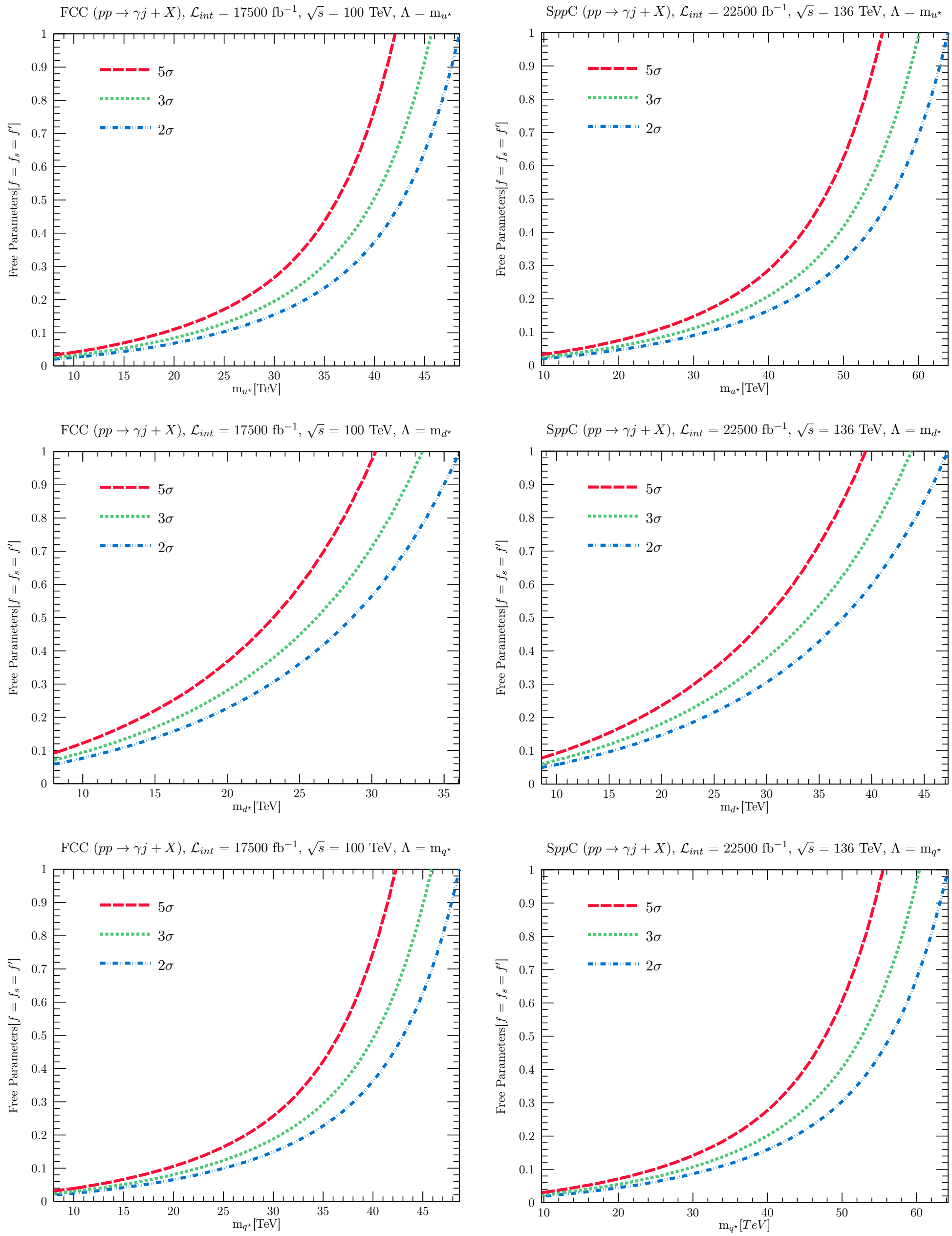

Fig. 8. Free parameters scan for excited quarks at FCC (left panel) and at S*pp*C (right panel).

are listed in Table 1, which reveals both colliders' physics potentials in terms of final luminosity values. At the end of FCC-Phase I operational time, the excited quarks discovery limit will be at 35.4 TeV. FCC-Phase II will make this discovery

Table 1. Attainable mass limits of excited quarks at FCC and SppC corresponding to integrated luminosity values by selecting $\Lambda = m_{Q^\star}$.

Colliders	FCC-Phase I			FCC-Phase II			SppC		
$\mathcal{L}_{\text{int}}$ (fb^{-1})	2500			17,500			22,500		
Significance	5σ	3σ	2σ	5σ	3σ	2σ	5σ	3σ	2σ
$m_{u^\star}$	35.1	38.8	41.7	42.1	45.7	48.5	55.2	60.1	64.0
$m_{d^\star}$ (TeV)	24.3	27.4	29.9	30.3	33.5	36.1	39.4	43.8	47.3
$m_{q^\star}$	35.4	39.0	41.9	42.3	45.9	48.7	55.5	60.4	64.2

Table 2. Achievable compositeness scale values for selected mass quantities for all three cases at FCC with final integrated luminosity values.

Mass (TeV)	Compositeness scale Λ (TeV) at FCC								
	$u^\star$			$d^\star$			$q^\star$		
	5σ	3σ	2σ	5σ	3σ	2σ	5σ	3σ	2σ
5.5	2559	4265	6398	796	1327	1991	2798	4663	6995
10	1564	2607	3911	429	716	1074	1690	2817	4226
20	485	808	1213	111	185	278	516	859	1289
30	162	270	406	31	52	77	165	275	412

Table 3. Achievable compositeness scale values for selected mass quantities for all three cases at SppC with final integrated luminosity values.

Mass (TeV)	Compositeness scale Λ (TeV) at SppC								
	$u^\star$			$d^\star$			$q^\star$		
	5σ	3σ	2σ	5σ	3σ	2σ	5σ	3σ	2σ
5.5	3631	6051	9077	1183	1972	2958	3913	6521	9781
10	2485	4142	6213	726	1210	1815	2646	4411	6616
20	988	1646	2469	248	413	620	1040	1733	2599
30	430	716	1074	96	160	239	449	748	1122
40	192	321	481	38	63	95	200	334	500

limit further up to 42.3 TeV. On the other hand, SppC with 22,500 fb^{-1} luminosity will take the discovery limits of $Q^\star$ up to 55.5 TeV.

Determining compositeness scale value is an important matter that could be decoupled of the excited quark mass, so this parameter can be scanned starting from the experimental mass limit of excited quark. Figure 7 provides attainable compositeness scale values of excited quarks at both energy frontier machines with their final luminosities. As can be seen from Fig. 7, degenerate cases held the highest compositeness scale values if the $m_{q^\star} = 5.5$ TeV: 2798 TeV (5σ), 4663 TeV (3σ) and

6995 TeV (2σ) at the FCC with $\mathcal{L}_{\rm int} = 17{,}500$ fb^{-1} and 3913 TeV (5σ), 6521 TeV (3σ) and 9781 TeV (2σ) at the SppC with $\mathcal{L}_{\rm int} = 22{,}500$ fb^{-1}. For some selected mass quantities, attainable compositeness scale values are listed in Tables 2 and 3.

The coupling constants are taken as $f = f_s = f'$ in order to reduce the number of parameters; up to now, we have chosen these three coupling constants equal to 1 however, these constants could be varied $0 < f,\ f_s,\ f' \leq 1$ (at least one of them must be different from zero). Their exact values are determined theoretically by given composite models.[38] Mass limits of excited quark at all confidence level are presented in Fig. 8, using both colliders' final luminosity values and taking $\Lambda = m_{Q^\star}$ for different coupling free parameters from around 0.1 up to 1. It is seen in Fig. 8, even free parameters are taken 0.1, degenerate case excited quark, $q^\star$, could be discovered at 19.4 TeV at FCC and 24.8 TeV at SppC.

The presented results show that FCC and SppC will have significant physics potential as new frontier machines. They will potentially discover excited quarks up to 42.3 TeV at FCC and 55.5 TeV at SppC. If excited quarks are discovered at these colliders, the compositeness scale of excited quarks will be determined.

Acknowledgments

TUBITAK supports this study under Grant No. 114F337. The authors are grateful to the Usak University, Energy, Environment and Sustainability Application and Research Center for their support. We also wish to acknowledge Assistant Prof. Yunus Emre Akbana for language editing and Dr. Hasan Eskalen for technical support.

References

1. M. Sahin, S. Sultansoy and S. Turkoz, *Phys. Rev. D* **83**, 054022 (2011).
2. J. C. Pati and A. Salam, *Phys. Rev. D* **10**, 275 (1974) [Erratum *ibid.* **11**, 703 (1975)].
3. M. Shupe, *Phys. Lett. B* **86**, 87 (1979).
4. H. Harari, *Phys. Lett. B* **86**, 83 (1979).
5. H. Terazawa, *Phys. Rev. D* **22**, 184 (1980).
6. H. Fritzsch and G. Mandelbaum, *Phys. Lett. B* **102**, 319 (1981).
7. H. Terazawa, M. Yasuè, K. Akama and M. Hayashi, *Phys. Lett. B* **112**, 387 (1982).
8. H. Terazawa, *Phys. Lett. B* **133**, 57 (1983).
9. E. J. Eichten, K. D. Lane and M. E. Peskin, *Phys. Rev. Lett.* **50**, 811 (1983).
10. I. A. D'Souza and C. S. Kalman, *Preons: Models of Leptons, Quarks and Gauge Bosons as Composite Objects* (World Scientific, 1992).
11. A. Çelikel, M. Kantar and S. Sultansoy, *Phys. Lett. B* **443**, 359 (1998).
12. M. E. De Souza, *Scientia Plena* **4** (2008).
13. H. Fritzsch, *Mod. Phys. Lett. A* **31**, 1630019 (2016), arXiv:1604.05818 [hep-ph].
14. A. Abada *et al.*, *Eur. Phys. J. Spec. Top.* **228**, 755 (2019).
15. F. Su, J. Gao, M. Xiao, D. Wang, Y.-W. Wang, S. Bai and T.-J. Bian, *Chin. Phys. C* **40**, 017001 (2016).
16. J. Gao, *Int. J. Mod. Phys. A* **32**, 1746003 (2017).
17. CEPC Study Group (M. Dong *et al.*), arXiv:1811.10545 [hep-ex].
18. CDF Collab. (F. Abe *et al.*), *Phys. Rev. Lett.* **74**, 3538 (1995).

19. DØ Collab. (V. M. Abazov *et al.*), *Phys. Rev. D* **74**, 011104 (2006).
20. DELPHI Collab. (J. Abdallah *et al.*), *Eur. Phys. J. C* **46**, 277 (2006).
21. CMS Collab. (S. Chatrchyan *et al.*), *Phys. Lett. B* **704**, 123 (2011).
22. CMS Collab. (V. Khachatryan *et al.*), *Phys. Lett. B* **738**, 274 (2014).
23. CMS Collab. (V. Khachatryan *et al.*), *Phys. Rev. Lett.* **116**, 071801 (2016).
24. CMS Collab., Search for excited quarks in the photon + jet final state in proton-proton collisions at 13 TeV, Technical Report CMS-PAS-EXO-16-015, CERN, Geneva (2016).
25. ATLAS Collab. (G. Aad *et al.*), *J. High Energy Phys.* **2016**, 41 (2016).
26. ATLAS Collab. (G. Aad *et al.*), *Phys. Lett. B* **754**, 302 (2016).
27. CMS Collab. (A. M. Sirunyan *et al.*), *Phys. Lett. B* **769**, 520 (2017).
28. CMS Collab., Search for excited states of light and heavy flavor quarks in the $\gamma+$jet final state in proton-proton collisions at $\sqrt{s} = 13$ TeV, Technical Report CMS-PAS-EXO-17-002, CERN, Geneva (2017).
29. ATLAS Collab. (M. Aaboud *et al.*), *Phys. Rev. D* **96**, 052004 (2017).
30. CMS Collab. (A. M. Sirunyan *et al.*), *J. High Energy Phys.* **2018**, 130 (2018).
31. CMS Collab. (A. M. Sirunyan *et al.*), *Phys. Lett. B* **781**, 390 (2018).
32. CMS Collab. (A. M. Sirunyan *et al.*), *Phys. Rev. D* **97**, 072006 (2018).
33. F. E. Low, *Phys. Rev. Lett.* **14**, 238 (1965).
34. H. Terazawa, Y. Chikashige and K. Akama, *Phys. Rev. D* **15**, 480 (1977).
35. L. Lyons, *Prog. Part. Nucl. Phys.* **10**, 227 (1983).
36. F. M. Renard, *Il Nuovo Cimento A* **77**, 1 (1983).
37. J. Kühn and P. Zerwas, *Phys. Lett. B* **147**, 189 (1984).
38. G. Pancheri and Y. Srivastava, *Phys. Lett. B* **146**, 87 (1984).
39. A. de Rújula, L. Maiani and R. Petronzio, *Phys. Lett. B* **140**, 253 (1984).
40. K. Hagiwara, S. Komamiya and D. Zeppenfeld, *Z. Phys. C* **29**, 115 (1985).
41. J. Kühn, H. Tholl and P. Zerwas, *Phys. Lett. B* **158**, 270 (1985).
42. U. Baur, I. Hinchliffe and D. Zeppenfeld, *Int. J. Mod. Phys. A* **02**, 1285 (1987).
43. M. Spira and P. Zerwas, *Heavy Flavours and High-Energy Collisions in the* 1–100 *TeV Range* (Springer, 1989), pp. 519–529.
44. U. Baur, M. Spira and P. M. Zerwas, *Phys. Rev. D* **42**, 815 (1990).
45. G. Jikia, *Nucl. Phys. B* **333**, 317 (1990).
46. F. Boudjema, A. Djouadi and J. L. Kneur, *Z. Phys. C* **57**, 425 (1993).
47. O. Çakır and R. Mehdiyev, *Phys. Rev. D* **60**, 034004 (1999).
48. O. Çakır, C. Leroy and R. Mehdiyev, *Phys. Rev. D* **62**, 114018 (2000).
49. O. Çakır, C. Leroy and R. Mehdiyev, *Phys. Rev. D* **63**, 094014 (2001).
50. O. J. P. Éboli, S. M. Lietti and P. Mathews, *Phys. Rev. D* **65**, 075003 (2002).
51. O. Çakır, A. Yılmaz and S. Sultansoy, *Phys. Rev. D* **70**, 075011 (2004).
52. O. Çakır, C. Leroy, R. Mehdiyev and A. Belyaev, *Eur. Phys. J. C* **32**, 1 (2004).
53. O. Çakır and A. Ozansoy, *Phys. Rev. D* **77**, 035002 (2008).
54. R. M. Harris and K. Kousouris, *Int. J. Mod. Phys. A* **26**, 5005 (2011).
55. S. Biondini, O. Panella, G. Pancheri, Y. N. Srivastava and L. Fanò, *Phys. Rev. D* **85**, 095018 (2012).
56. H. Terazawa and M. Yasuè, *J. Mod. Phys.* **05**, 205 (2014).
57. H. Terazawa and M. Yasue, *Nonlin. Phenom. Complex Syst.* **19**, 1 (2016), arXiv:1508.00172 [hep-ph].
58. S. Biondini and O. Panella, *Phys. Rev. D* **92**, 015023 (2015).
59. O. Panella, R. Leonardi, G. Pancheri, Y. N. Srivastava, M. Narain and U. Heintz, *Phys. Rev. D* **96**, 075034 (2017).
60. A. Caliskan, S. O. Kara and A. Ozansoy, *Adv. High Energy Phys.* **2017**, 1 (2017).
61. A. Caliskan, *Adv. High Energy Phys.* **2017**, 1 (2017).

62. Y. O. Günaydin, M. Sahin and S. Sultansoy, *Acta Phys. Polon. B* **49**, 1763 (2018), arXiv:1707.00056 [hep-ph].
63. U. Kaya, B. B. Oner and S. Sultanoy, *Turk. J. Phys.* **42**, 235 (2018), arXiv:1707.08897 [hep-ph].
64. A. Caliskan and S. O. Kara, *Int. J. Mod. Phys. A* **33**, 1850141 (2018).
65. A. N. Akay, Y. O. Günaydin, M. Sahin and S. Sultansoy, *Adv. High Energy Phys.* **2019**, 1 (2019).
66. A. Belyaev, N. D. Christensen and A. Pukhov, *Comput. Phys. Commun.* **184**, 1729 (2013), arXiv:1207.6082 [hep-ph].
67. A. V. Semenov, arXiv:hep-ph/0208011.
68. A. Semenov, *Comput. Phys. Commun.* **201**, 167 (2016), arXiv:1412.5016 [physics. comp-ph].
69. J. Pumplin, D. R. Stump, J. Huston, H.-L. Lai, P. Nadolsky and W.-K. Tung, *J. High Energy Phys.* **2002**, 012 (2002).
70. D. Stump, J. Huston, J. Pumplin, W.-K. Tung, H.-L. Lai, S. Kuhlmann and J. F. Owens, *J. High Energy Phys.* **2003**, 046 (2003).
71. K. Gumus, N. Akchurin, S. Esen and R. M. Harris, CMS sensitivity to dijet resonances, Technical Report (2006).